

NOVEL NANOMETER SCALE CONSTITUENT ELECTROCERAMIC THIN FILMS FOR THE NEXT GENERATION OF ARMY COMMUNICATION SYSTEMS

M.W. Cole*, C. Hubbard, E. Ngo, W. Nothwang, M. Bratcher, M. Ervin and M. Wood
U.S. Army Research Laboratory
Aberdeen Proving Ground, MD 21005

R.G. Geyer
National Institute of Standards and Technology, RF Technology Division
Boulder, CO 80305

ABSTRACT

The influence of low concentration (1 mol%) Mg-doping on the structural, microstructural, surface morphological and dielectric properties of $Ba_{1-x}Sr_xTiO_3$ (BST) thin films has been measured and analyzed. The films were fabricated on MgO and Pt-Si substrates via the metalorganic solution deposition technique using carboxylate-alkoxide precursors and postdeposition annealed at 800 °C (film/MgO substrates) and 750 °C (film/Pt-Si substrates). The structure, microstructure, surface morphology and film/substrate compositional quality were analyzed by glancing angle x-ray diffraction, field emission scanning microscopy, atomic force microscopy and Auger electron spectroscopy studies. Dielectric properties of unpatterned films were measured at 10 GHz using a coupled, tuned split dielectric resonator system, and at 100 kHz using metal-insulator-metal capacitors. The Mg-doped BST films exhibited improved dielectric and insulating properties compared to the undoped $Ba_{0.6}Sr_{0.4}TiO_3$ thin films. The improved dielectric properties, low leakage current, and good dielectric tunability of the low level Mg-doped BST thin films merits strong potential for utilization in microwave tunable devices for FCS.

1. INTRODUCTION

Antennas, “the spinal cord for weapons and communications systems”, remain one of the most critical communication components for enabling information dominance, situational awareness, lethality, survivability, and enhanced mobility of future land forces in the 21st century. The Army’s future combat system (FCS) antennas require increased bandwidth for multimission communications; increased antenna gain for robust communications and range extension; increased mobility for high data rate on-the-move (OTM) communications; and undetectable antenna visual signatures for low probability of mission detection and increased survivability. Electronic scanning antennas (ESA’s) are the key components for such advanced communication systems. ESA’s provide rapid scanning

capability, which enables modes such as multiple target tracking, track while scan and sensor fusion operation. One of the major challenges, which must be overcome before such advanced ESA systems can be realized, is the development of affordable, low loss, high tunability, low power, lightweight, and high performance microwave frequency phase shifters. The enabling technology for such phase shifters is centered on the development of single-phase nano-scale constituent electroceramic thin films with enhanced dielectric, insulating, and microstructural properties.

Thin films of $Ba_{1-x}Sr_xTiO_3$ (BST) have recently received considerable attention as promising candidates for applications in tunable electronically controllable microwave devices, such as voltage tunable phase shifters, capacitors, oscillators, filters and parametric amplifiers (Chang et al., 1999; Zafar et al., 1998). These tunable devices are based on a large field dependent dielectric constant, which results in a change in phase velocity in the device, allowing it to be tuned in real time for a particular application (Cole et al., 2000). For the realization of such tunable devices at microwave frequency it is important to develop a paraelectric thin film material with low microwave loss, high tunability, and good insulating properties. To date, thin film BST which simultaneously possesses both low loss at microwave frequency and a large tunability as required for many microwave applications has not been realized. It is well documented that small concentrations of acceptor dopants can dramatically modify the properties, i.e., lower dielectric loss, of ferroelectric materials such as BST (Joshi and Cole, 2000). In particular, Fe^{2+} , Fe^{3+} , Co^{2+} , Co^{3+} , Mn^{2+} , Mn^{3+} , Ni^{2+} , Mg^{2+} , Al^{3+} , Ga^{3+} , In^{3+} , Cr^{3+} , and Sc^{3+} , which can occupy the B sites of the $(A^{2+}B^{4+}O_2)_3$ perovskite structure, have been known to lower dielectric loss (Joshi and Cole, 2000; Horwitz et al., 1998; Wu et al., 1998). Recently, the Army Research Laboratory has successfully designed, fabricated, characterized, and optimized, novel pure and acceptor doped $Ba_{0.6}Sr_{0.4}TiO_3$ (BST) based thin films with excellent microwave material properties. In this paper we evaluate the process-structure-property relationships and report the microwave dielectric properties for pure

and 1 mol% Mg doped BST thin films prepared via the metalorganic solution deposition technique.

2. EXPERIMENTAL

Undoped and 1 mol% Mg doped Ba_{0.6}Sr_{0.4}TiO₃ thin films were fabricated by the metalorganic solution deposition (MOSD) technique. Ba acetate, Sr acetate, and Ti isopropoxide were used as precursors to form BST. Acetic acid and 2-methoxyethanol were used as solvents and magnesium acetate was employed as the dopant precursor. The precursor films were spin coated onto Pt-coated silicon and (100) single crystal MgO substrates. Particulates were removed from the solution by filtering through 0.2 μm syringe filters. Subsequent to coating, the films were pyrolyzed at 350 °C for 10 min. in order to evaporate solvents and organic addenda and form an inorganic amorphous film. The spin coat pyrolyzation process was repeated until a nominal film thickness of 165 nm was achieved. Crystalline films were achieved via postdeposition annealing in an oxygen ambience at 750 °C and 800 °C, for the films deposited on the Pt-silicon and MgO substrates, respectively.

The films were characterized for dielectric, insulating, structural, compositional, interfacial, and surface morphological properties. The dielectric properties were characterized utilizing both unpatterned microwave and low frequency capacitor measurement techniques. The microwave dielectric properties were measured at 10 GHz using unpatterned undoped and Mg doped BST thin films grown on MgO substrates via a coupled/split dielectric resonator system (SDRS). Figure 1 displays a schematic diagram of the split dielectric resonator system. This measurement technique is noncontacting and nondestructive. The measurement capabilities of this technique are currently from 1 – 30 GHz. The sample insertion gap is determined by making the azimuthal electric field in the gap as uniform as possible at the nominal measurement frequency.

The general measurement procedure is to identify and measure the TE_{01δ} resonant frequency and unloaded Q factor of the split dielectric resonator system without and with specimen insertion. The Rayleigh-Ritz variational method is used to compute the resonant frequencies and unloaded Q factors as a function of permittivity and geometry of the tuned split dielectric resonators and parametrically as a function of specimen real permittivity ϵ_r' and specimen thickness t . A lookup table is established that enables the real part of the permittivity to be determined iteratively from

$$\epsilon_r' = 1 + (f_0 f_s) / [t f_0 F(\epsilon_r', t)], \quad (1)$$

where f_0 and f_s are the resonant frequencies of the SDRS without specimen insertion and with specimen insertion

and $F(\epsilon_r', t)$ is a numerically determined parametric function of ϵ_r' and t . Since this technique makes use of the dominant TE_{01δ} mode, which has only an azimuthal electric field component, the electric field is continuous across the dielectric interfaces and in-plane sample properties are measured. The electric field continuity also makes the resonant system insensitive to the presence of axial air gaps between specimen and the two tuned dielectric resonators. The specimen dielectric loss tangent, $\tan \delta_s$, is evaluated from

$$\tan \delta_s = p_{e,s}^{-1} [Q_o^{-1} - p_{e,DR} \tan \delta_{DR} - Q_c^{-1}], \quad (2)$$

where Q_o is the unloaded Q factor of the resonant system containing the inserted specimen, $\tan \delta_{DR}$ is the dielectric loss tangent of the cylindrical dielectric resonators of the fixture, Q_c^{-1} denotes fixture conductor losses for the resonant system containing the specimen, and $p_{e,s}$, $p_{e,DR}$ are the partial electronic energy filling factors of the specimen and the split dielectric resonators of the system. The sample partial electric energy filling factor is defined as the electric energy in the sample normalized by the electric energy in the entire resonant system

$$p_{e,s} = \iiint_{V_s} \epsilon_{r,s} \mathbf{E} \cdot \mathbf{E}^* dv / \iiint_V \epsilon_r \mathbf{E} \cdot \mathbf{E}^* dv, \quad (3)$$

where \mathbf{E} is the azimuthal electric field defined over the volume V . The partial electric energy filling factor in the split dielectric resonators is similarly defined. Fixture conductor losses are defined in terms of the metal surface resistance R_s and the magnetic field \mathbf{H} evaluated over the volume and surface of the resonant system

$$Q_c^{-1} = R_s \iint_S \mathbf{H}_t \cdot \mathbf{H}_t^* dS / \iiint \mu_0 \mathbf{H} \cdot \mathbf{H}^* dv. \quad (4)$$

For unpatterned thin films, the measurement process is two-fold. First, the permittivity and dielectric loss of the substrate is evaluated. Then the permittivity and dielectric loss of the thin film are determined by the resonant frequency and Q -factor differences between substrate and substrate with deposited thin film. For a single substrate measurement, the relative uncertainty in specimen real permittivity, $\Delta \epsilon_{r,s}' / \epsilon_{r,s}'$ depends on the uncertainties in thickness and diameter of the dielectric resonators, the diameter of the enclosing circular waveguide, the insertion gap, and the specimen thickness. Generally, the total estimated uncertainty is dominated by the uncertainty of the sample under test and is given by

$$\Delta \epsilon_{r,s}' / \epsilon_{r,s}' = T \Delta t / t, \quad (5)$$

where $1 < T < 2$. Usually T is close to unity except for thick, large permittivity samples. The relative dielectric loss tangent uncertainty of a single-layer specimen having real permittivity less than 10 is less than 4 % for loss tangents in excess of 0.001, provided Q -factor measurements are performed with a measurement

uncertainty that is less than 1%. For the thin film measurements reported here, the relative thin film dielectric loss tangent uncertainty, $\Delta \tan \delta_{tf} / \tan \delta_{tf}$, is given by the following weighted rms sum of the uncertainties in partial filling factors of the thin film, substrate, and dielectric resonators in resonant system, as well as the uncertainties in metal quality-factor, unloaded Q -factor, and substrate and dielectric resonator loss tangents:

$$\begin{aligned} \Delta \tan \delta_{tf} / \tan \delta_{tf} = & [(S_{pe,tf} \Delta p_{e,tf} / p_{e,tf})^2 + (S_{Q0} \Delta Q_0 / Q_0)^2 \\ & + (S_{Qc} \Delta Q_c / Q_c)^2 + (S_{pe,DR} \Delta p_{e,DR} / p_{e,DR})^2 \\ & + (S_{pe,substrate} \Delta p_{e,substrate} / p_{e,substrate})^2 \\ & + (S_{\tan \delta, substrate} \Delta \tan \delta_{substrate} / \tan \delta_{substrate})^2 \\ & + (S_{\tan \delta, DR} \Delta \tan \delta_{DR} / \tan \delta_{DR})^2]^{1/2}, \end{aligned} \quad (6)$$

where

$$S_{pe,tf} = 1, \quad (7)$$

$$\begin{aligned} S_{Q0} = & 1 + p_{e,DR} \tan \delta_{DR} / (p_{e,tf} \tan \delta_{tf}) + p_{e,substrate} \\ & \times \tan \delta_{substrate} / (p_{e,tf} \tan \delta_{tf}) + 1 / (Q_c p_{e,tf} \tan \delta_{tf}), \end{aligned} \quad (8)$$

$$\begin{aligned} S_{pe,substrate} = & S_{\tan \delta, substrate} = p_{e,substrate} \\ & \times \tan \delta_{substrate} / (p_{e,tf} \tan \delta_{tf}), \end{aligned} \quad (9)$$

$$S_{pe,DR} = S_{\tan \delta, DR} = p_{e,DR} \tan \delta_{DR} / (p_{e,tf} \tan \delta_{tf}), \quad (10)$$

and

$$S_{Qc} = 1 / (Q_c p_{e,tf} \tan \delta_{tf}). \quad (11)$$

Thin film real permittivity is based on the measured frequency shift between substrate and substrate with deposited film. This frequency shift is determined by the contrast in permittivity between the film and substrate and film thickness, which affects the film electric energy filling factor. The upper bound uncertainty in frequency measurement with an Automatic Network Analyzer (ANA) is 1 kHz. Hence the systematic uncertainty in thin film real permittivity evaluation is dominantly related to thickness uncertainties in either the substrate or thin film.

Variations in frequency shift between substrate and substrate with deposited thin film are given in Fig. 2 for thin film permittivities that vary from 100 to 500 and for thin film thicknesses that range from 50 nm to 500 nm. These computations were performed assuming a MgO substrate having a real permittivity of 9.75 and thickness of 0.50 mm. As the film thickness becomes smaller for a given film real permittivity, the frequency shift decreases, as does the partial electric energy filling factor in the film. By measuring both the substrate and thin film thickness variations, frequency shift differences

such as those shown in Fig. 2 may be used for rapid determination of the systematic uncertainty in a specimen's real permittivity evaluation. The films tested here were 165 nm thick with a thickness uncertainty of 2 nm. For the measurements reported here, the total relative uncertainty in ferroelectric film permittivity is principally controlled by the substrate thickness uncertainty, and is estimated to be 5%. The dominant contribution to the uncertainty in thin film loss tangent is that arising from errors in unloaded Q -factor and in fixture metal quality factor. For typical uncertainties in the partial filling factors of the dielectric resonators, substrate, and thin film, and for loss tangents of the dielectric resonators and substrate and metal surface resistance, the total estimated uncertainty in thin film dielectric loss tangent for measurements reported here is 20% for 2% accuracy in unloaded Q -factors.

The low frequency (100 kHz) dielectric and insulating measurements were conducted on the undoped and Mg-doped BST thin films deposited on Pt-Si substrates in the metal-insulator-metal (MIM) capacitor configuration. The film capacitance (C_p) and dissipation factor ($\tan \delta$) were measured with an HP 4194A impedance/gain analyzer. The insulating properties of the films were evaluated via I-V measurements using a HP 4140B semiconductor test system. The film crystallinity was assessed via glancing angle x-ray diffraction (GAXRD) using a Rigaku diffractometer with CuK α radiation at 40 kV. Cross-sectional film microstructure was examined using a Hitachi S4500 field emission scanning electron microscope (FESEM). The surface morphology of the films was assessed by a Digital Instrument's Dimension 3000 atomic force microscope (AFM) using tapping mode. The elemental distribution within and across the film-substrate interface was assessed using a Perkin-Elmer 660 scanning Auger microscope.

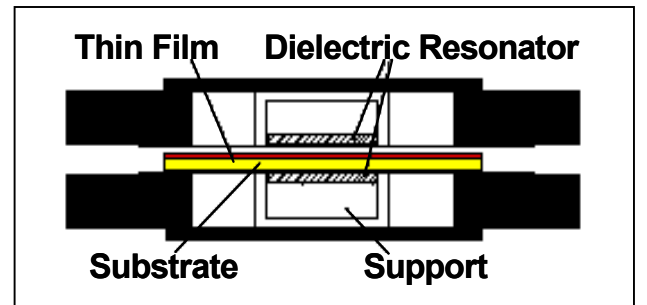


Figure 1. Schematic diagram of the split dielectric resonator system

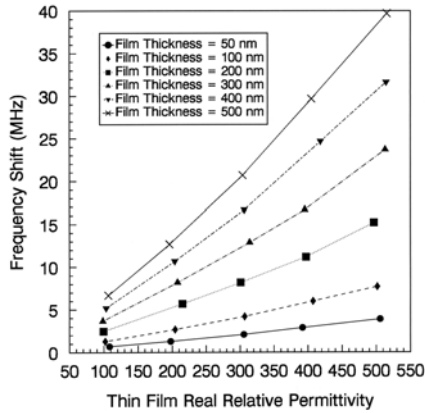


Figure 2. Frequency shift of split dielectric resonator system between substrate and substrate with thin film as function of film real permittivity and thickness.

3. RESULTS AND DISCUSSION

Pure and 1 mol% Mg doped BST thin films were fabricated by the metalorganic solution deposition (MOSD) technique using carboxylate-alkoxide precursors. The film's dielectric properties were characterized at microwave frequency via a tuned coupled-split dielectric resonator technique. Using this measurement technique, for first time ever, has allowed the true "sole" dielectric loss ($\tan \delta$) and permittivity (ϵ_r) of the BST-based films to be assessed and optimized without the influence of device design (radiative losses) and electrode metallization (conductor losses). The thin film dielectric properties are summarized in Table I.

TABLE I. Dielectric and insulating properties of the pure and 1 mol% Mg doped BST thin films.

Sample	freq.	ϵ_r (0 bias)	$\tan \delta$ (0 bias)	tunability % (300kV/cm)	$\rho \times 10^{12}$ (Ω -cm)
BST/MgO	10 GHz	406	0.025	---	---
1 mol% Mg- BST/MgO	10 GHz	348	0.022	---	---
BST/PtSi	100 kHz	450	0.013	50.1	0.40
1 mol% Mg- BST/PtSi	100 kHz	423	0.009- 0.01	43.0	0.55

The data tabulated in Table I demonstrates that amounts as low as ~1 mol% of the Mg dopant have a noticeable influence on the dielectric and insulating properties of the thin films. The 1 mol% Mg-doped BST thin film possessed a lower dielectric loss and permittivity than that of the undoped BST thin film. The real permittivity for both the undoped and 1 mol% Mg-doped thin films, at both frequencies, is reasonable (less than 500) for device impedance matching purposes, thereby allowing efficient power transfer in the device (Saha and Krupanidhi, 2000; Cole et al., 2001). The electrical quality, that is, the insulating nature, of a dielectric film is determined by the value of leakage

current, converted to resistivity, in Table I. Thus, the insulating/resistivity thin film data are an electrical measure of the quality and reliability of a dielectric film (Cole et al., 2000; Saha and Krupanidhi, 2000). The Mg-doped BST film possessed an enhanced film resistivity value (low leakage current) with respect to that of the undoped BST thin film. The film resistivity of the 1 mol% Mg doped BST was ~1.4 times larger than that of the undoped BST. Capacitance-voltage measurements were used to analyze the effect of Mg doping on the dielectric tunability of the BST films. The dielectric tunability (in %) is defined in terms of $\Delta C/C_o$, where ΔC is the change in capacitance relative to zero-bias capacitance C_o . The tunability, measured at 300 kV/cm, was found to decrease with the addition of the Mg dopant. Considering the tradeoffs between tunability and the values of dielectric loss, permittivity, and film resistivity, the 1 mol% Mg-doped BST film possessed better overall material properties with respect to that of undoped BST for tunable device applications. The enhanced material properties, bode well for the utilization of Mg doped BST thin films in phase shifter device components. It is well known that the variations in the dielectric properties of the BST based material system are strongly influenced by sample composition, crystallinity, grain size, stress, and the quality of the film-substrate interface (Tsai et al., 1997; McNeal et al., 1988) Therefore, in order to fully evaluate and mechanistically understand the dielectric and insulating properties tabulated in Table I the influence of the Mg dopant on the structural, microstructural, interfacial, and surface morphological properties was evaluated and correlated with the films dielectric and insulating properties.

The as-pyrolyzed BST-based thin films were amorphous and postdeposition annealing was required to impart crystallinity, increase the overall grain size of the film, and to remove film strain by filling oxygen vacancies. These factors are particularly important because the dielectric loss in ferroelectric thin films is strongly influenced by stoichiometric deficiencies, which create vacancies, film strain, and the presence of a large grain boundary to grain ratio (Cole et al., 2000; Horwitz et al., 1998). Therefore, in order to reduce the microwave loss the as-pyrolyzed films were post-deposition annealed for 1h in the temperature range of 600 to 800 °C in an oxygen ambience. Glancing angle x-ray diffraction was utilized to assess film crystallinity and to determine whether or not the films possessed a single phase structure. Figure 3 displays the GAXRD patterns of the undoped and 1 mol% Mg doped BST films deposited on MgO substrates. The absence of diffraction peaks in the x-ray diffraction patterns for both film compositions annealed at 600 °C indicated that these films were amorphous in nature. Partially crystallized undoped and Mg-doped films were obtained at an

annealing temperature of 650 °C with no evidence of secondary phase formation. As the annealing temperature was increased the x-ray peak intensity increased and the full-width-half-maximum (FWHM) decreased indicating enhanced crystallinity and an increase in grain size with increasing annealing temperature up to 800 °C. The 800 °C annealed undoped and doped films were single phase, cubic, and possessed a non-textured polycrystalline structure. Direct comparison of the GAXRD data for the undoped and doped films showed that the FWHM of the Mg doped film was larger than that of the undoped BST films at all annealing temperatures indicating a smaller grain size for the Mg doped BST films with respect to that of the undoped films. For both film compositions there was a slight shift of the x-ray peak positions to lower angles with respect to that of bulk BST. The lattice parameter for the film annealed at 650 °C, $a_{(T=650)} = 4.0249 \text{ \AA}$, was slightly larger than that for the 800 °C annealed film $a_{(T=800)} = 3.9759 \text{ \AA}$. Thus, as the film was annealed at higher temperatures the lattice parameter contracted approaching the bulk BST value of $a_{(\text{BST } 60/40)} = 3.9655 \text{ \AA}$. The presence of oxygen vacancies is known to increase the lattice parameter of oxide films, therefore this noted lattice parameter contraction implies a decrease in oxygen vacancy concentration as the annealing temperature approached 800 °C, thereby improving the film quality. This low oxygen vacancy concentration, in response to postdeposition annealing in an oxygen ambience at 800 °C is reflected in the excellent resistivity values (Table I) for both film compositions. Leakage current values are strongly influenced by film growth parameters, microstructure, and the density of oxygen vacancies in the film (Cole et al., 2000; Horwitz et al., 1998; Wu and Barnes, 1998).

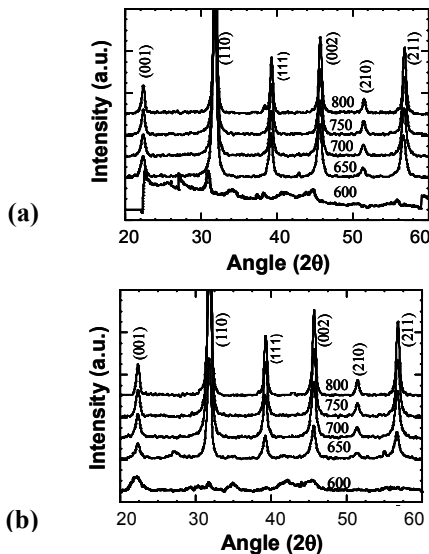


Figure 3. X-ray diffraction patterns of the (a) undoped and (b) 1 mol% Mg doped BST films.

The surface morphology of the films was assessed

via tapping mode AFM over a $1 \times 1 \mu\text{m}^2$ scan area. The AFM images of the films annealed at 800 °C, displayed in Fig. 4, show that both the undoped and Mg-doped films exhibited a dense microstructure with no cracks or defects observed. The surface roughness, as quantified by AFM, was found to increase with increasing annealing temperature resulting in an average surface roughness (R_{av}) of 2.25 nm at 800 °C for both film compositions. The parameter of film surface roughness is extremely important for device performance since the dielectric properties depend not only on a well-defined microstructure, but also on the quality the electrode (required for microwave devices)-film interface. A smooth film surface, of the order of 2.25 nm, will promote intimate contact between the film and electrode metallization, i.e., a sharp film-electrode interface, resulting in a lower conductor loss as compared to a rough film surface. It has been reported that surface roughness has a strong influence on the value of leakage current or film resistivity (Hwang et al., 2001; Sugii and Rakagi, 1998), thus, the fact that the undoped and Mg doped MOSD films are extremely smooth is consistent with the excellent film resistivity values reported in Table I. The AFM results demonstrated that the Mg dopant had no appreciable affect on the films surface roughness; however, the AFM results did show a grain size difference between the annealed undoped and doped films. Figure 5 displays a plot of grain size as a function of annealing temperature for both the undoped and Mg doped films. The results support the GAXRD findings suggesting that even a small amount of Mg dopant added to BST depresses the grain size relative to that of undoped BST. This result was also observed for 5 mol% Mg doped films deposited on Pt-Si substrates (Cole et al., 2000). The grain size for the fully crystallized undoped and Mg doped films was 75 nm and 67 nm, respectively.

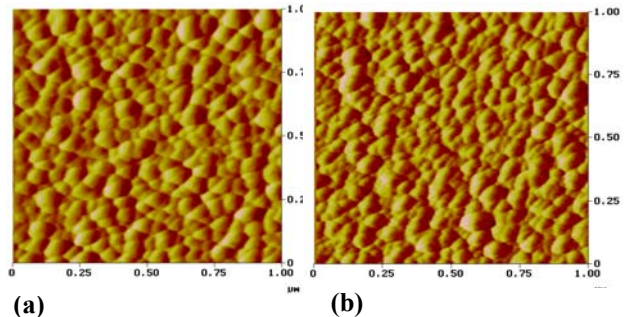


Figure 4. AFM micrographs of the (a) undoped BST and (b) 1 mol % Mg doped BST film surfaces postdeposition annealed at 800 °C

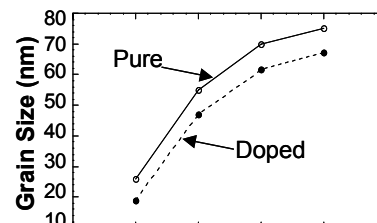


Figure 5. Grain size (determined via AFM) as a function of annealing temperature for both film compositions on MgO substrates.

The permittivity of a ferroelectric/paraelectric film is strongly influenced by grain structure, grain size, and quality of the material throughout the volume of the film. A larger grain size results in a larger polarization, hence, higher permittivities are expected for larger grain size materials. The permittivity increases with increasing grain size since the volume of dielectric polarization is proportional to the size of the grain. Thus, the smaller grain size of the Mg doped film with respect to that of the undoped BST film is most likely responsible for its lower permittivity value (Table I) observed at both low and microwave frequencies. The decrease in tunability with the addition of the 1 mol% Mg dopant is explained by the fact that the T_c is lower for the Mg doped films (Cole et al., 2000; Joshi and Cole, 2000). It is known that the dielectric tunability increases near the T_c (Wu and Barnes, 1998). The fact that the tunability measurements were obtained at room temperature for both film compositions combined with the observed temperature down-shift in T_c for the Mg doped film explains the slightly lower tunability for the Mg doped film relative to the undoped BST film.

The films microstructure, in the direction perpendicular to the film growth, was analyzed via cross-sectional FESEM. The cross-sectional FESEM micrographs of the 800 °C annealed films (not shown) demonstrated that both films possessed a dense well-crystallized microstructure with a uniform cross-sectional thickness of 165 nm. The films were polycrystalline and were composed of granular multigrains randomly distributed through out the film thickness. The FESEM micrographs showed a distinct structural delineation between the film and the MgO substrate. No amorphous layer or voiding/defects was observed at the film-MgO interface. This defect free and structurally abrupt interface bodes well for the excellent mechanical integrity and good adhesion characteristics of the undoped and Mg doped BST film-MgO substrate.

The Auger electron spectroscopy (AES) depth profiles of the undoped and 1 mol% Mg doped BST films are displayed in Fig. 6. The AES elemental depth profiles revealed a sharp interface with no interdiffusion of constituent elements between the dielectric film and

the MgO substrate. The depth profiles also revealed that each element component of the film possessed a uniform distribution from the film surface to the film-substrate interface. These data substantiate the fact that the undoped and Mg doped BST films on MgO substrates maintain chemical and thermal stability at processing temperatures up to 800 °C (annealing temperature). The fact that no impurities were observed in the AES elemental depth profile, without doubt, contributed to the films good dielectric and insulating properties.

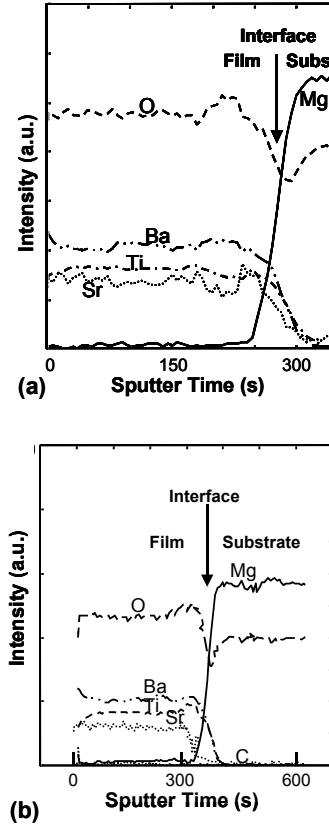


Figure 6. AES elemental depth profiles of the 800 °C annealed (a) undoped and (b) 1 mol% Mg doped $Ba_{0.6}Sr_{0.4}TiO_3$ thin films on MgO. The elemental signals in the AES spectra are delineated by a solid line (—) for Mg, small dotted line (····) for Sr, large dotted line (·····) for C, dashed-dotted line (- · - ·) for Ti, a large dashed line (— —) for O, and a dash followed by two dots (- · ·) for Ba.

Results of this investigation have demonstrated that Mg doping as low as 1 mol% had a notable influence on the films microstructure, dielectric, and insulating properties. The exact mechanism by which Mg altered the film properties is not fully understood. The fact that the films were deposited on the same type of substrate, processed via the same chemical fabrication technique,

and crystallized under the same annealing conditions (time, temperature, and ambience) suggests the influence of induced film stress arising from lattice mismatch ($a_{\text{MgO}}=4.213 \text{ \AA}$ and $a_{\text{BST}(60/40)}=3.947 \text{ \AA}$) and the difference in thermal expansion coefficients ($\alpha_{\text{MgO}}=13.8 \times 10^{-6}/^{\circ}\text{C}$ and $\alpha_{\text{BST}(60/40)}=10.5 \times 10^{-6}/^{\circ}\text{C}$) between the film and substrate were not the primary cause of the observed dielectric property modifications. We suggest that the Mg doping (composition alteration) is the parameter, which is responsible for the modification of the BST thin film material properties. Material doping has been reported to modify and control thin film dielectric and insulating properties by reducing the oxygen vacancy concentration (Gopalan et al., 1999; Moos and Hardtl, 1996). Acceptor-type dopants can prevent the reduction of Ti^{4+} to Ti^{3+} , by neutralizing the donor action of the oxygen vacancies. Because the electrons resulting from the generation of oxygen vacancy can hop between different titanium ions and provide a mechanism for dielectric losses, the compensation for oxygen vacancy with the correct amount of acceptor dopant such as Mg^{2+} , should in theory, help to lower the loss tangent. The difference in dielectric loss between the Mg doped film and undoped BST film was small (~ 0.003), but noteworthy. It must be kept in mind that the concentration of the Mg dopant was extremely low, only 1 mol %, thus its effect on dielectric loss is notable but somewhat understated. We suggest that the differences in dielectric loss would diverge further, improving the dielectric loss with higher Mg dopant concentrations up to the point of structural phase segregation. We further speculate that the Mg dopant served to enhance the insulation resistance (excellent film resistivity values listed in Table I) of the BST based film, by suppressing the concentration of oxygen vacancies, and growth of potential barrier at grain boundaries. As a final comment, It must be noted, that microstructural differences, such as, the grain size reduction in the 1 mol% doped BST film with respect to undoped BST, may have altered the film's stress field, which in turn may also have contributed to the modification of films dielectric properties.

4. CONCLUSIONS

This investigation demonstrated that Mg doping as low as 1 mol% had a noteworthy influence on the material properties of BST thin films. The annealed undoped and 1 mol% Mg-doped BST films were single phase, possessed a dense defect free microstructure with a thermally stable film-substrate interface, and smooth continuous surface morphology. Improved dielectric and insulating properties were achieved for 1 mol% Mg-doped BST thin films with respect to that of pure BST films. The 10 GHz measured values of dielectric constant and dissipation factor of BST thin films doped

with 1 mol% Mg were 348 and 0.022, respectively. The film resistivity was also enhanced as a result of the Mg doping. The compensation for oxygen vacancies via low amounts of Mg acceptor doping was suggested to be responsible for the enhanced material properties of the 1 mol% Mg doped BST thin film. Thus, the enhanced material properties of Mg doped MOSD fabricated BST thin films merits strong potential for utilization in phase shifters, thereby allowing the communication effectiveness required for combat-ready FCS electronic scanning antenna's to be realized.

REFERENCES

- Chang, W., Horwitz, J.S., Carter, A.C., Pond, J.M., Kirchoefer, S.W., Gilmore, C.M., and Chrisey, D.B., "The Effect of Annealing on the Microwave Properties of $\text{Ba}_{0.5}\text{Sr}_{0.5}\text{TiO}_3$ Thin Films," *Appl. Phys. Lett.*, Vol 74, No. 7, pp.1033-1035, February 1999.
- Cole, M.W., Joshi, P.C., Ervin, M.H., Wood, M.C, and Pfeffer, R.L., "The Influence of Mg Doping on the Materials Properties of $\text{Ba}_{1-x}\text{Sr}_x\text{TiO}_3$ Thin Films For Tunable Device Applications," *Thin Solid Films*, Vol 374, pp.34-41, October 2000.
- Cole, M.W., Joshi, P.C., Ervin, M.H., "La Doped $\text{Ba}_{1-x}\text{Sr}_x\text{TiO}_3$ Thin Films For Tunable Device Applications," *J. Appl. Phys.*, Vol 89, No.11, pp. 6336-6340, June 2001.
- Gopalan, S., Wong, C-H, Balu, V., Lee, J.-H., Han, J. H., Mohammedali, R., and Lee, J., "Effect of Niobium Doping on the Microstructure and Electrical Properties of Strontium Titanate Thin Films for Semiconductor Memory Application," *Appl. Phys. Lett.*, Vol 75, No. 14, pp. 2123-2125, October 1999.
- Horwitz, J.S., Chang, W., Carter, A.C., Pond, J.M., Kirchoefer, S.W., Chrisey, D.B., Levy, J., Hubert, C., "Structure/Property Relationships in Ferroelectric Thin Films For Frequency Agile Microwave Electronics," *Integr. Ferroelectrics*, Vol 22, pp. 279-289, October 1998.
- Hwang, C-C, Juang, M.-H., Lai, M.-J., Jaing, C.-C., Chen, J.-S., Huang, S., Cheng, H.-C., "Effect of Rapid-Thermal Annealed TiN Barrier Layer on the Pt/BST/Pt Capacitors Prepared by RF Magnetron Co-Sputter Technique at Low Substrate Temperature," *Solid State Electronics*, Vol 45, No.1, pp. 121-125, January 2001.
- Joshi, P.C. and Cole, M.W., "Mg-Doped $\text{Ba}_{0.6}\text{Sr}_{0.4}\text{TiO}_3$ Thin Films for Tunable Microwave Applications " *Appl. Phys. Lett.*, Vol 77, No. 2, pp. 289-291, July 2000.
- McNeal, M.P., Jang, S.J., and Newman, R.E., "The Effect of Grain and Particle Size on the Microwave

- Properties of Barium Titanate (BaTiO_3),” *J. Appl. Phys.*, Vol 83, No. 6, pp. 3288-3297, March 1988.
- Moos, R and Hardtl, K.H., “Electronic Transport Properties of $\text{Sr}_{1-x}\text{La}_x\text{TiO}_3$ Ceramics” *J. Appl. Phys.*, Vol 80, No. 1, pp. 393 –400, July 1996.
- Saha, S. and Krupanidhi, K.B., “Impact of Microstructure on the Electrical Stress Induced Effects of Pulsed Laser Ablated (Ba,Sr) TiO_3 Thin Films,” *J. Appl. Phys.*, Vol 87, No.6, pp. 3056-3062, March 2000.
- Sugii, N., and Rakagi, K., “Change in Surface Morphologies with Pulsed-Laser –Deposition-Temperature for SrTiO_3 and $\text{Ba}_{0.7}\text{Sr}_{0.3}\text{TiO}_3$ Thin Films on Pt Electrodes” *Thin Solid Films*, Vol 323, pp. 63-67, June 1998.
- Tsai, M.S., Sun, S.C., and Tseng, T.Y., “Effect of Oxygen to Argon ratio on Properties of (Ba,Sr) TiO_3 Thin Films Prepared by Radio-Frequency Magnetron Sputtering” *J. Appl. Phys.*, Vol 82, No7, pp. 3482 – 3487, October 1997.
- Wu, H.-D. and Barnes, F.S., “Doped $\text{Ba}_{0.6}\text{Sr}_{0.4}\text{TiO}_3$ Thin Films For Microwave Device Applications at room temperature,” *Integr. Ferroelectrics*, Vol 22, pp. 291-305, October 1998.
- Zafar, S., Jones, R. E., Chu, P., White, B., Jiang, B., Taylor, D., Zurcher, P. and Gillepsie, S., “Investigation of Bulk and Interfacial Properties of $\text{Ba}_{0.5}\text{Sr}_{0.5}\text{TiO}_3$ Thin Film Capacitors,” *Appl. Phys. Lett.*, Vol 72, No. 22, pp. 2820-2822, June 1998.